Spin relaxation in mesoscopic superconducting Al wires

Yun-Sok Shin,[*] Hu-Jong Lee,[†] and Hyun-Woo Lee

Department of Physics, Pohang University of Science and Technology, Pohang 790-784, Republic of Korea

(Dated: February 2, 2008)

We studied the diffusion and the relaxation of the polarized quasiparticle spins in superconductors. To that end, quasiparticles of polarized spins were injected through an interface of a mesoscopic superconducting Al wire in proximity contact with an overlaid ferromagnetic Co wire in the single-domain state. The superconductivity was observed to be suppressed near the spin-injecting interface, as evidenced by the occurrence of a finite voltage for a bias current below the onset of the superconducting transition. The spin diffusion length, estimated from finite voltages over a certain length of Al wire near the interface, was almost temperature independent in the temperature range sufficiently below the superconducting transition but grew as the transition temperature was approached. This temperature dependence suggests that the relaxation of the spin polarization in the superconducting state is governed by the condensation of quasiparticles to the paired state. The spin relaxation in the superconducting state turned out to be more effective than in the normal state.

Recently the spin-dependent electron transport has been the subject of intensive studies. The key element of the phenomenon is to inject a current of spin-polarized conduction electrons into a mesoscopic or nano-scale non-magnetic metal or semiconductor, control, and detect the resulting spin state. Spin-polarized electron can be injected from a ferromagnet (F) into the system under study.[1,2,3,4,5,6,7,8] To realize the spin-dependent electronic conductance or "spintronics" it is essential to obtain the accurate information on the characteristic spin-relaxation time or length of the injected electrons in the metallic or semiconducting system in the presence of spin-relaxing scattering.[1,2,3,4,5,6,7,8] The spin-relaxation originates from both scattering by magnetic impurities and spin-orbit scattering of conduction electrons, but the relaxation due to spin-orbit scattering is dominant without magnetic impurities. A number of studies on the spin relaxation in metals have been done using nonlocal spin injection,[1,8,9] conduction electron spin resonance,[10,11,12] weak localization,[13,14] and superconducting tunneling spectroscopy.[15,16,17,18] Observed spin relaxation rate using different techniques at room temperature, where the electron-phonon interaction predominates the spin-orbit scattering, reveals reasonable consistency, but it shows a wider spread at low temperatures around liquid helium temperature. It has been pointed out that[9], as the impurity scattering predominates the spin-orbit scattering at low temperatures, the measured spin relaxation rates may depend on different measurement techniques which are sensitive to different impurity-induced spin-orbit scattering.

Recently, the spin relaxation in a superconductor (S), both conventional[19,20,21,22,23,24] and high-T_c cuprate,[25,26,27,28] has attracted much research interest in relation with the recombination mechanism of the spin-polarized quasiparticles into the singlet Cooper-paired state. A number of studies on the spin diffusion in conventional superconductors, however, have revealed contradicting results. Measurements of spin accumulation effect in F/S/F-type bipolar spin transistors[19] showed an increase of the spin-diffusion length in superconducting Nb films as $\lambda_{sp}(T) = \lambda_{sp}(0)/(1 - T/T_c)^n$ with $1/4 < n < 1/2$, with increasing temperature below the superconducting transition temperature T_c. But this result was in contradiction to the increase of the spin-relaxation rate with increasing temperature near T_c from below in superconducting Nb films and potassium-doped fulleride (K_3C_{60}) compounds measured by the electron spin resonance technique.[20,21] More recent theoretical studies by Yamashita *et al.*,[22] however, indicated that the estimated spin-diffusion length in both the superconducting state (neglecting the charge imbalance effect) and the normal-metallic state should be the same, implying that the spin-diffusion characteristics should be independent of temperature in the narrow temperature range below T_c.

On the other hand, studies on the influence of the spin-polarized quasiparticle injection into high-T_c cuprates[25,26,27,28] have mainly been focused on the effective suppression of the superconductivity. The sensitive dependence of the critical current on the spin injection in a low-carrier-density cuprate hybridized with a highly polarized colossal magnetoresistance material is expected to open a way to develop active three-terminal superconducting devices with a high current gain. In addition, it is expected that the spin injection into cuprates may provide key information on the possible roles of the spin degrees of freedom in bringing about the high-T_c superconducting order. For these purposes also clear understanding of the spin relaxation mechanism in the cuprates is an essential element.

In this study we injected a spin-polarized current from a ferromagnetic Co wire into a mesoscopic superconducting Al wire which was in proximity contact with the Co wire and observed the resulting suppression of the superconductivity

in the Al wire. In general, the superconductivity suppresses as superconducting pairs are broken by the injection of the nonequilibrium quasiparticles into a superconductor. In our study with the injection of a spin-polarized current into a superconducting wire through the F/S interface, the superconductivity was more effectively suppressed as the time-reversal symmetry of the superconducting pairs in the singlet state was easily broken in the nonequilibrium state. We estimated the spin-diffusion length λ_{sp} from the finite voltages revealed in the Al wire for a bias below the onset current of superconductivity (for convenience we assign this as the superconducting critical current), which itself was reduced by the weakened superconductivity due to spin-polarized current injection. The resulting spin-diffusion length saturated at temperatures far below T_c but grew gradually with increasing temperature and tended to diverge near T_c. This result is consistent with the results of Ref. 19 but is in contradiction to the results of Refs. 20-22. The detailed temperature dependence of λ_{sp} in our study indicated that the spin relaxation in a superconductor was related to the condensation of quasiparticle pairs in two opposite spin channels into superconducting electron pairs at the Fermi level.

Specimens were fabricated using a combination of electron-beam (e-beam) lithography, e-beam and/or thermal evaporation, Ar-ion etching, and lift-off techniques. Si substrates covered with natural oxide layers were used. For F/S hybrid samples (the samples A and B) ferromagnetic wires designed to form in a single-domain structure[29] were made by the e-beam evaporation of 60~65-nm-thick Co films on patterned layers of e-beam resist and by lifting off subsequently to the width of about 250~270 nm. Then about 80~130-nm-thick Al layers for both samples with extended contact electrodes were thermally evaporated as superconducting wires on the second patterned resist and lifted off to the width of about 200 nm and 270 nm, respectively. There was about 10% variation in the width of the Al wire over the length under study for both samples. The surface of the ferromagnetic layers was cleaned using low-energy Ar-ion milling right before the Al deposition to enhance the transparency of the Co/Al interface. To compare the results between the spin-polarized and spin-degenerate configurations, a control sample C was fabricated by the same method as described above, in which, however, the ferromagnetic Co wire was replaced by a non-magnetic Au wire.

Schematic configuration of the samples is shown in Fig. 1(a). The Al wire, with multiple voltage leads, was in crossed contact with a ferromagnetic Co wire. The total number of segments of the Al wires was 6, 9, and 6 for the samples A, B, and C, respectively. For the nonequilibrium spin injection into the superconducting Al wire the current was applied between the leads A and D. But for the injection of spin-degenerate nonequilibrium quasiparticles the leads C and D were used. Pair-breaking of superconducting electrons due to the injection of the spin-polarized current was monitored by measuring the $I-V$ characteristics of each segment of an Al wire between two neighboring voltage leads. For the sample A, the voltage drop in the segments of the Al wire V_1, V_2, $\cdots$, V_6 was monitored between the leads C and E, E and F, $\cdots\cdots$, I and J, respectively, as shown in Fig. 1(b). The sample C had the same nominal geometry as the sample A. For the sample B the voltage drop V_1, V_2, $\cdots\cdots$, V_9 was also monitored between the leads B and E, E and F, $\cdots\cdots$, L and M, respectively, as shown in Fig. 1(c) in detail. The center-to-center length of the segment corresponding to the voltage drop V_1 (the segment one) was 460 nm (1.6 μm) and the average center-to-center spacing between the adjacent voltage leads for other segments was 340~380 nm (1.8 μm) for the samples A and C (B).

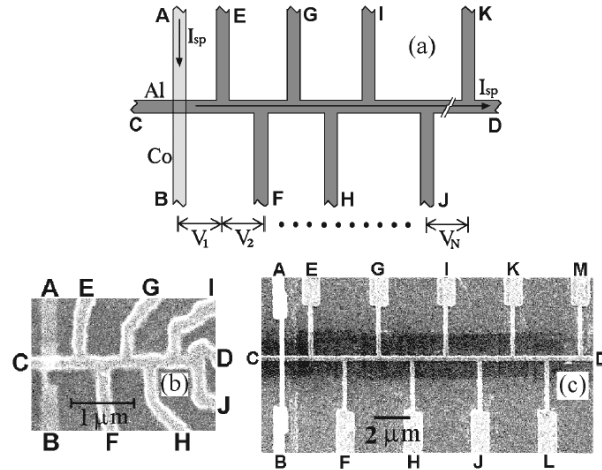Data were taken by the conventional four-probe lock-in technique run at 38 Hz in a dilution refrigerator. The

FIG. 1: (a) Schematic geometry of the samples. SEM micrographs of (b) the sample A and (c) the sample B.

diffusion constant D of Al wire at 4.2 K, determined from the wire residual resistivity, was 12.0 (24.8) cm^2/s for the sample A (B). To obtain the value of D, we used the relation[30] for Al $\rho l_e = 3.2 \times 10^{-12}$ Ωcm^2, where ρ and l_e are the resistivity and the elastic mean-free path, respectively, of the Al wires in the normal state. Here, the value of the Fermi velocity for Al[31] $v_F = 2.03 \times 10^8$ cm/s was used. The interfacial resistance R_t for the sample A (B, C) was about 2.4 (2.4, 0.04) Ω far below the superconducting transition temperature T_c of Al. The corresponding interfacial transparency t of the sample A (B, C), 0.22% (0.15%, 11%), was determined using the relation[32] of $R_t^{-1} = 2N(E_F)v_F Se^2 t$. Here, $N(E_F)$ and v_F are the density of states at the Fermi level and the Fermi velocity of Co (Au), respectively, for the samples A and B (C). S and e are the cross-sectional area of the interface and the electron charge, respectively.

In Fig. 2 the resistance vs temperature of the Al wire of the sample A, determined by measuring the voltage drop $V_{1(2,6)}$ between the leads C (E, I) and E (F, J), is shown for a spin-polarized bias current I_{sp} of 1 μA, applied between the leads A and D. One notes that no interfacial resistance was included in the data in this measurement configuration. Since the sample A has a defect in the lead B near the interface [see Fig. 1(b)] this lead was not used in the measurements. The voltage drop in the segment which is closest to the interface (the segment one), V_1, shows much smeared characteristics below the onset of the superconducting transition T_c than those in other segments (the segments two and six) such as V_2 or V_6 in the figure. The voltage drops V_3, V_4, and V_5 over other segments showed behavior (not illustrated in the figures) very similar to V_2 with a few % deviation of the onset temperatures of zero resistance. The finite resistance corresponding to V_1 in the segment one below the onset of the superconducting transition is most likely to be due to weakening of the superconductivity in the Al wire by the spin-polarization-induced pair breaking. The open-circle symbols are the data with the current bias of 1 μA for the spin-degenerate bias configuration over the segment one, where the voltage drop for the unpolarized spin injection is almost identical to that for the case of the spin injection. This fact indicates that the nonequilibrium effect of quasiparticle injection is supposed to be minimal for this low bias level.

On the other hand, the identical results between the two bias configurations imply that, even for this quasi-equilibrium situation in the low spin-degenerate bias current, pair breaking comparable to the level for corresponding spin injection takes place. Random interdiffusion of conduction electrons even without an external bias current can take place crossing the interface. This, in turn, induces spin accumulation in the Al wire near the interface, because the spin population of the two opposite polarities is imbalanced in the ferromagnetic Co wire. The resulting spin acclumulation in the superconducting Al wire induces the pair breaking and causes the finite resistance below the bulk transition temperature T_c of Al. Thus, the finite resistance below T_c of the Al wire is not due to the bias-induced pair breaking but is due to the self spin injection near the interface. This is similar to the "self injection" effect as discussed in Ref. 27. The difference in the normal-state resistance for different segments resulted from the variation in the length as well as in the width of segments. The unusual peak in the resistance corresponding to V_1 is presumably due to nonuniform current distribution at the junction as the Al electrode became superconducting. This peak feature appeared even in the Au/Al junction of the sample C.
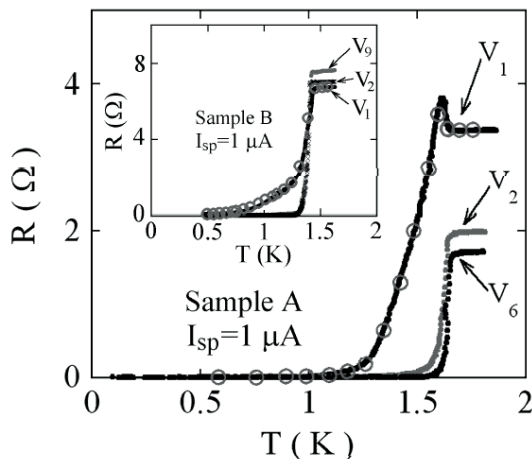

FIG. 2: The resistive transition of the Al wire of the sample A for different segments corresponding to the voltage drop V_1, V_2, and V_6 in Fig. 1 for the bias current of 1 μA in the spin-injection configuration. Open circles are the data corresponding to the spin-degenerate configuration. Inset: the temperature dependence of the Al-wire resistance of the sample B for the bias current of 1 μA along the segments one, two, and nine in the spin-injection configuration (solid curves) and along the segment one in the spin-degenerate configuration (open circles).

As illustrated in the inset of Fig. 2 similar behavior was observed in the wire resistance vs temperature of the sample B for the segments represented by V_1, V_2, and V_9. For the sample B also the open-circle data corresponding to V_1 for the spin-degenerate bias configuration are almost the same as those for the spin injection configuration. This indicates again that the bias level of 1 μA used to determine the temperature dependence of resistance of the sample B was low enough so that the equilibrium electron state in the Al wire was not disturbed even for the spin-injection bias configuration. The spatial dependence of the resistance in Fig. 2 also reveals that the spin-polarized state of the bias current was confined within the segment one of the Al wire in both samples.

The behavior of the Al-wire resistance that was almost insensitive to the bias between spin-injection and spin-degenerate configurations changed for higher current biases. The inset of Fig. 3 shows again the resistance vs temperature of the segment one of the Al wire of the sample A for increasing spin-polarized bias current from 1 to 15 μA. For the bias of 10 μA a finite resistance appeared even below the original value of T_c, which indicates that, for this bias level, significant spin-polarization-induced pair breaking took place. For 15 μA almost full pair breaking is visible. In comparison, for the spin-degenerate bias configuration, the resistive transition of the Al wire for the samples A and B remained almost unaltered for the current bias up to 15 μA (the data are not shown). On the other hand, when we injected a current through a nonmagnetic Au wire, no noticeable pair breaking effect was visible up to 15 μA for any bias modes. Fig. 3 shows such resistive transition for the segment one of the Al wire of the sample C. In this sample consisting of Au/Al junction the transition of the segment one of the Al wire is much sharper than in the previous case consisting of Co/Al interface. Apparently in this case no pair breaking due to spin accumulation effect dominated the resistive-transition characteristics of the Al wires.

Fig. 4 shows the spatial dependence of the $I-V$ characteristics of the segments one, two, three, and six of the sample A measured at 0.10 K in the spin-polarized bias configuration. The voltage value of each segment is normalized with respect to the normal-state resistance. Except for small variation the segments two, three, and six show transition to the normal state at corresponding critical currents with almost equal sharpness. In contrast, the transition of the segment one is much smeared with a significantly reduced critical current. The appearance of the clear finite resistance in the segment one below its critical current is due to the pair breaking by the spin injection. As observed in the resistive-transition data in Fig. 2, the spatial variation of the $I-V$ curve also indicates that the spin injection effect decays within the range comparable to the length of the segment one of superconducting Al wire.

In the inset of Fig. 4 we also illustrate the spatial dependence of the spin injection effect exhibited in the $I-V$ characteristics of the sample B. Different sets of $I-V$ characteristics were taken from the segments one, two, $\cdots$, and nine[33] at 0.43 K. For clarity, each set is offset downward from the neighboring curve by 0.03 mV. In this sample also the finite voltage below the critical current is present only for the segment one, which is consistent with the picture that it was caused by the pair breaking due to the nonequilibrium spin injection within the spin-diffusion length near the interface.

The inset of Fig. 5 clearly contrasts with the $I-V$ characteristics of the segment one of the sample A measured at 0.1 K between the two different configurations: the grey curve shows the characteristics for the spin-injection configuration and the black curve is the one without spin injection. For the spin-injection configuration the $I-V$ curve is much smeared with a significantly reduced critical current. The slightly peaked feature in the voltage near
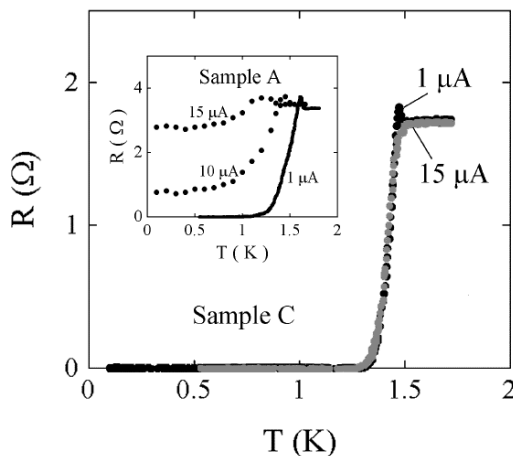

FIG. 3: The resistive transition for the segment one of the Al wire of the sample C, consisting of a Au/Al junction, for the bias currents of 1 and 15 μA. Inset: the resistive transition of the segment one of the Al wire of the sample A for increasing spin-polarized bias current from 1 to 15 μA.

the critical current above the normal-state value in the spin-injection configuration is not well understood. But the feature appeared only in the segment one so that one may assume it was caused by nonuniform current distribution at the junction.

We took the nonequilibrium conduction properties of the Al wire in a sample where the ferromagnetic Co wire was replaced by non-magnetic normal wire, *i.e.*, the sample C. In this case the injected current was spin degenerate in any bias configurations. In the main panel of Fig. 5, $I - V$ characteristics of the segment one of the control sample C are compared between biasing through leads A and D as denoted by I_{Au} and biasing through leads C and D as denoted by I_{Al}, which would correspond to the spin-polarized and spin-degenerate mode, respectively, for the samples A and B. $I - V$ characteristics turn out to be almost identical in both bias configurations, because pair breaking due to spin injection was absent in both cases. Slight discrepancy between the two curves arose from the possible difference in the effective length of the segment one between the two configurations and/or the nonuniform current distribution at the interface for the bias current of I_{Au}. Even for this spin-degenerate configuration, however, pair breaking by the nonequilibrium current injection may have smeared the superconducting transition of the Al wire near the critical current as seen in the figure.

One may argue that the seeming spin-injection effect was caused by simple Joule heating generated by a bias current in the ferromagnetic wire or at the interface. In fact, the control sample C where the seeming spin-injection effect was absent had a interfacial resistance much lower than the samples A and B with Co/Al interfaces. In order to interpret the suppression of superconductivity described above in terms of spin-related pair breaking one need to rule out the possibility of thermally induced pair breaking effect. To examine the possibility of Joule heating at the interface conduction properties of Al wire in a sample with much higher interfacial resistance were measured. Fig. 6 shows the differential resistance measured in another test sample at temperatures far below T_c, over three different distances from the interface. The junction area of this sample was similar to that of the rest of the samples and the interfacial resistance of this sample was 17.4 Ω, almost an order of magnitude higher than the samples A and B. One notices that all the curves, including the one for the segment one that is closest from the interface, have similar sharpness of the transition with almost the same values of the critical current. If there were significant contribution of heating at the interface the segment one should show much smeared characteristics with a reduced critical current. The behavior of the curves in this figure indicates that the heating effect is supposed to be insignificant even for a junction with resistance much higher than those of the samples A and B. On the other hand, in this test sample with higher interfacial resistance, the spin injection is supposed to be ineffective because of the spin flip scattering at the interface. Thus, the spin injection effect was not present in the data of Fig. 6. This argument indicates that the appearance of finite voltages below the critical currents in the spin-injection configuration, in the samples A and B, resulted from pair breaking due to spin injection to the Al wires both with the relatively low interfacial resistance of 2.4 Ω.

We estimate the effective spin diffusion length λ_{sp} from the finite voltages below the critical current by adopting a phenomenological model. Suppose a superconducting wire is placed along the x axis with the F/S interface at x=0. In the model, local superconducting gap $\Delta_s(x, T)$, in the presence of the spin accumulation near the interface
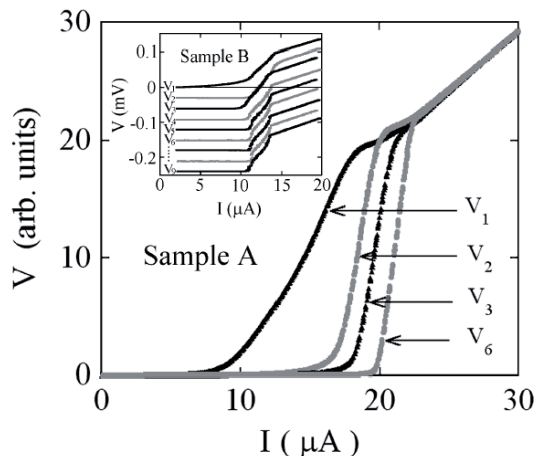

FIG. 4: $I - V$ characteristics of the sample A taken at 0.10 K, along the segments one, two, three, and six of the Al wire for the spin-injection bias configuration. Inset: the spatial dependence of the $I - V$ characteristics taken from the segments 1, 2, ..., 9 of the Al wire of the sample B at 0.43 K. For clarity each curve is offset downward from the nearest neighbor by 0.03 mV.

of F/S, is assumed to be $\Delta_0(T) - A|P(x,T)|$ for $\Delta_0(T) > A|P(x,T)|$ and zero otherwise. Here, $\Delta_0(T)$ is the local superconducting gap in the absence of the spin accumulation, $|P(x,T)|$ is the absolute density of the spin imbalance, and A is a parameter defined as (a dimensionless constant)$\times 1/N_n$, where N_n is the density of states per unit volume in the normal state. The local critical current $I_c(x,T)$ is assumed to be $B\Delta_s(x,T)$, where B is another parameter defined as (a dimensionless constant)$\times N_n e v_F \times$(the cross section of a superconducting wire). Then, the voltage drop V over a region of Al wire of length L from the interface for an applied current I is given by

$$
\begin{aligned}
V &= \int_0^L dx \frac{\Delta V}{\Delta x} \\
&= \int_0^L dx I R_n \frac{1}{L} \theta(I - I_c(x,T)) \\
&= I R_n \frac{1}{L} \int_0^L dx \theta(I - I_c(x,T)) \\
&= I R_n \frac{L_n^{eff}}{L},
\end{aligned}
\tag{1}
$$

where $\theta(y)$ is the step function, which is 1 for $y > 0$ and 0 otherwise. Here, R_n and L_n^{eff} are the resistance of the Al wire and the effective spin diffusion length in the normal state, respectively. The total voltage drop V is the sum of the local voltage drop ΔV over an infinitesimal segment Δx. The local voltage drop ΔV appears when the applied bias current I exceeds the local critical current $I_c(x,T)$ of an infinitesimal segment Δx located at x. From the assumption above, the critical current $I_c(L_n^{eff}, T)$ is determined by the relation $I_c = B[\Delta_0(T) - A|P(L_n^{eff}, T)|]$. If the local density of spin accumulation is assumed to relax exponentially as $P(x,T) = P_0(T)\exp[-x/\lambda_{sp}(T)]$ the effective spin diffusion length follows the relation, $L_n^{eff} = \lambda_{sp}\log[ABP_0/(B\Delta_0 - I)]$. Hence, the voltage drop V is obtained as

$$
\begin{aligned}
V &= 0, \quad \text{for } 0 < I < B\Delta_0 - ABP_0 \\
&= I R_N, \quad \text{for } I > B\Delta_0 \\
&= I R_N \frac{\lambda_{sp}}{L} log[\frac{ABP_0}{B\Delta_0 - I}], \quad \text{otherwise.}
\end{aligned}
\tag{2}
$$

This relation is satisfied for a strong superconducting state with large $\Delta_0(T)$ in the temperature range sufficiently below T_c. In this case the spatial distribution of the superconducting strength may look like the one as illustrated in the inset of Fig. 7(a). As the temperature approaches T_c, however, a certain range over the length L_n of the Al wire from the interface loses the superconductivity with vanishing $\Delta_s(x,T)$ as Δ_0 becomes smaller than
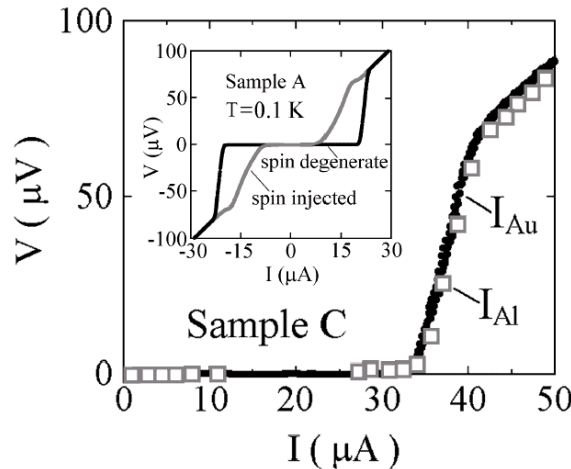

FIG. 5: $I - V$ characteristics for the segment one in the control sample C (consisting of Au/Al junction), taken at 0.10 K for the bias current fed from Au lead (solid circle) and from Al lead (open square), which would correspond to spin-polarized and spin-degenerate configurations, respectively, in the samples A and B. In the inset the $I - V$ characteristics for the segment one in the sample A at 0.10 K in the spin-injection configuration (the grey curve) in comparison with the spin-degenerate bias configuration (the black curve).

$A|P(x,T)|$ near T_c [see the inset of Fig. 7(b)]. Then, the spatial dependence of $P(x,T)$ for $x > L_n$ is modified as $P_0(T)\exp[-L_n/\lambda_n(T)]\exp[-(x-L_n)/\lambda_{sp}(T)]$. Here, L_n and λ_n are the length of normal region for $\Delta_0 < A|P(x,T)|$ and the spin diffusion length in the normal state, respectively. The ratio of L_n/L is assumed to be proportional to the ratio between the zero-bias-limit resistance and the normal-state resistance near T_c. In this case, the voltage drop V is also modified as

$$
\begin{aligned}
V &= IR_n\{\frac{L_n}{L} + \frac{\lambda_{sp}}{L}log[\frac{ABP_0'}{B\Delta_0 - I}]\}, \text{ for } 0 < I < B\Delta_0 \\
&= IR_n, \text{ otherwise.}
\end{aligned}
\tag{3}
$$

where, $P_0' = P_0(T)\exp[-L_n/\lambda_n(T)]$.

Using Eqs. (2) and (3), the spin diffusion lengths far below T_c and near T_c are extracted, respectively. We adopted three fitting parameters λ_{sp}, ABP_0 and $B\Delta_0$ for the best fit to Eq. (2). ABP_0 should be less than $B\Delta_0$ and the value $B\Delta_0 - ABP_0$ is the maximum bias current of the zero-resistance state in the temperature regime far below T_c. On the other hand, we adopted two parameters λ_{sp} and ABP_0' for the best fit to Eq. (3). The value of ABP_0 must be larger than $B\Delta_0$ in the temperature range near T_c. In the fit the value of ABP_0 near T_c is extracted from the value of the quantity for $T \ll T_c$ as obtained in the fit to Eq. (2), while assuming a linear temperature dependence. $B\Delta_0$ near T_c is also determined from its value far below T_c incorporated with the BCS-type temperature dependence of the energy gap, $\Delta_0(T)$.[34]

As discussed in relation with Eq. (2), $I-V$ curves at 0.10 K in the sample A show the three different characteristic regimes of voltage drop V for a range of bias current I: the zero resistance regime, the finite-voltage regime below the critical current and the normal resistance regime above the critical current. In the finite-voltage regime, the three fitting parameters, $\lambda_{sp} = 340$ nm, $ABP_0 = 14$ μA and $B\Delta_0 = 20$ μA at 0.10 K, are determined from the best fit (solid line) to the $I-V$ curves in Fig. 7(a). It turns out, however, that the quality of the best-fit curve is not much sensitive to the fitting parameter values within 10 % of variation. The resulting best-fit parameter values give the relative magnitudes among parameters that are consistent with the assumptions given above. In comparison, in Fig. 7(b), the $I-V$ curves at 1.3 K show two regimes of voltage drop V: the finite-voltage regime below the critical current and the normal-resistance regime above the critical current. The features in Figs. 7(a) and 7(b) are consistent with the assumed variation of the superconducting strength as illustrated in their insets in relation with Eqs. (2) and (3), respectively. The length of normal-state region L_n at 1.3 K, as estimated from the zero-bias-limit resistance, is 48 nm. The best-fit values (solid line) of the parameters turn out to be $\lambda_{sp} = 410$ nm and $ABP_0' = 11$ μA. In this fit we used the local gap value, corresponding to $B\Delta_0 = 13.7$ μA , obtained from the BCS behavior.

The value $ABP_0 = 11.2$ μA at 1.3 K, which is obtained by linearly extrapolating the low-temperature-limit values as obtained from the fit in relation with Fig. 7(a), is not in agreement with the assumption of $ABP_0 > B\Delta_0$. This contradiction presumably originates from the naive assumptions of step function in Eq. (1) and/or the linear dependence between the critical current and the energy gap. One may believe that the existence of the zero-bias-limit
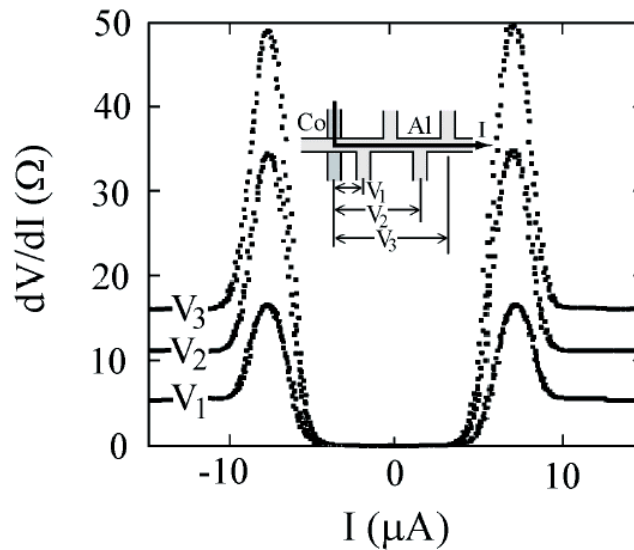

FIG. 6: The differential resistance measured in a test sample consisting of Co/Al interface at temperatures far below T_c over three different distances from the interface.

resistance implies $\Delta_s = 0$ at the interface, but the fitting formula of Eq. (3) may hold only approximately in the intermediate temperature range between 0 and T_c. The fit, following the same procedure, to $I - V$ characteristics far below T_c and near T_c for the sample B gave similar quality of the fit (not shown).

In Fig. 8 we plot the temperature dependence of λ_{sp} extracted from the best-fit to $I - V$ characteristics. It shows that the spin diffusion length λ_{sp} is almost temperature independent in the temperature range far below T_c, which is 1.6 K (1.56 K) for the sample A (B). The zero-temperature-limit value of $\lambda_{sp}(0)$ for the sample A (B) was 340 nm (400 nm). The empirical value of λ_{sp} increases with T and tends to diverge near T_c. This temperature dependence of λ_{sp} turns out to be in remarkable agreement with that observed in the c-axis spin-polarized quasiparticle tunneling in YBa$_2$Ca$_3$O$_{7-\delta}$ thin films.[27] The temperature dependence of λ_{sp} is also in qualitative agreement with the results obtained in Nb[19] but in clear contradiction with result in Refs. 20 and 21, where λ_{sp} decreases for temperatures approaching T_c. The temperature dependence of λ_{sp} also contradicts to the theoretical results of Ref. 22, where the spin-diffusion length is predicted to be the same both in the normal and in the superconducting states, implying that the spin diffusion length in a superconductor should be almost independent of temperature in the range of our study.

The spin diffusion length in the normal state in our study is estimated to be $\lambda_n \sim 1$ μm from the ratio between the extrapolated value of $P_0(T)$ and the fitting parameter of $P_0'(T)$, with 50 % variation in its value in the temperature range near T_c where the assumption of $ABP_0 > B\Delta_0$ is satisfied. Thus, the temperature dependence of λ_n cannot be accurately determined near T_c. The spin relaxation time in the normal-metallic state τ_n in the sample A(B) is calculated to be about 450 (1170) ps at 1.4 K using the relation of $\lambda_n = \sqrt{D\tau_n}$, which is in comparison with the previous results[8] for τ_n of 100 ps at 4.2 K obtained using the nonlocal spin-injection measurements.

Employing the picture of the relaxation of charge-imbalanced nonequilibrium quasiparticle states in a superconductor,[35] the spin relaxation time has been suggested to follow the relation,[27]

$$\tau_{sp} \sim \tau_{ex} k_B T_c / \Delta(T). \tag{4}$$

Here, the energy-relaxation time or the inelastic-scattering time τ_{ex} is defined in terms of the spin exchange as
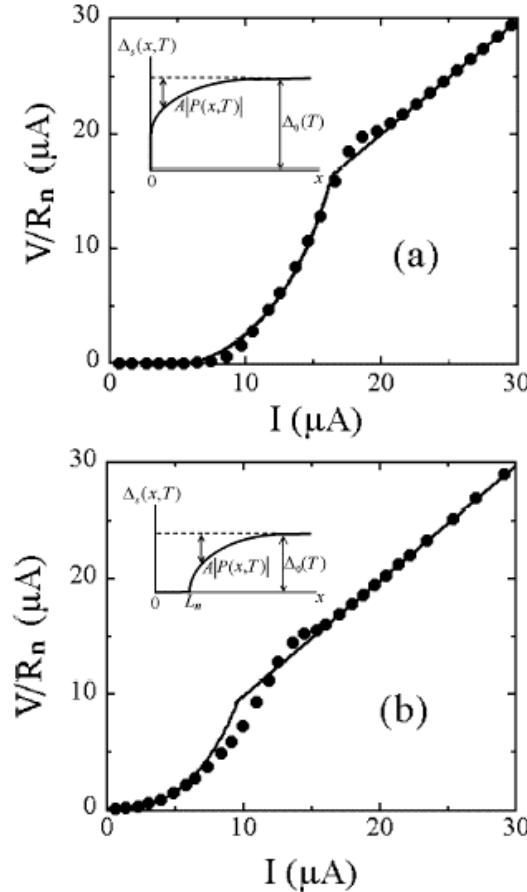

FIG. 7: $I - V$ characteristics (open circles) of the segment one for temperatures (a) far below T_c ($T = 0.1$ K) (b) and near T_c ($T = 1.3$ K) in the sample A, with the best-fit curves (solid curve) using Eqs. (2) and (3).

$\tau_{ex} \sim \hbar/h_{ex}$ (h_{ex} is the exchange energy inside the superconductor) and $\Delta(T)$ is the superconducting energy gap. In this picture, the nonequilibrium spin imbalance is set by the characteristic energy-relaxation or inelastic scattering time but only the fraction of quasiparticles $\delta/k_B T_c$ just above the gap is effectively involved in relaxing the spin imbalance.[35] Then temperature dependence of the spin diffusion length, expressed as $\lambda_{sp} = \sqrt{D\tau_{sp}}$, should be determined by the temperature dependence of Δ as $1/\sqrt{\Delta(T)}$. The best fit to this temperature dependence is shown for the samples A and B in Fig. 8 by solid curves. In the fit we use the empirical formula[34] $\Delta(T) = \Delta(0)\tanh(1.74\sqrt{T_c/T - 1})$ for the temperature dependence of the gap, which is supposed to be valid in all the temperature range below T_c [=1.6 (1.56) K], with T_c as the fitting parameter for the sample A (B). Combining $\lambda_{sp}(0)= 340$ (400) nm with D=12.0 (24.8) cm^2/sec for the sample A (B), the spin relaxation time in the Al wire for $T \ll T_c$ is estimated to be $\tau_{sp} \sim 9.6$ (6.5) $\times 10^{-11}$ sec for the sample A (B). The corresponding exchange energy h_{ex}/k_B for the sample A (B) was 91 mK (95 mK), which is larger than the value of 11 mK for Nb.[19] The fast spin relaxation, corresponding to the large exchange energy, in Al was discussed in Ref. 9, in terms of the pseudopotential band calculation results by Fabian and Das Sarma.[36] It is theoretically suggested that the small spin hot spots at the large Fermi surface of polyvalent metals like Al give excessive contribution to the spin flip scattering, making the spin relaxation faster by up to a factor of 100. The nice fit of the temperature dependence of λ_{sp}, on the other hand, indicates that the spin diffusion in superconductors is governed by the energy relaxation between the opposite spin channels as well as the pair condensation over the superconducting gap.

The spin-relaxation length measured previously in the normal state of Al[9] at 4.2 K was 1200 nm, which is thus longer than that in the superconducting state by a factor of ~ 4 as measured in this study. Although the direct comparison of the spin diffusion lengths in systems with different electron diffusivity is meaningless the above trend may indicate that the spin diffusion length in the normal state is, in general, longer than that in the superconducting state. One may explain this trend in terms of plausible spin-relaxation processes in superconducting system in the following way. An imbalanced nonequilibrium state of the spin-polarized quasiparticles between the opposite spin bands in the superconductor, caused by the spin injection, relaxes to a non-equilibrium spin-balanced state, which in turn relaxes to the equilibrium condensed Cooper-paired state. The (second) recombination process in a superconductor depopulates the quasiparticles in the nonequilibrium state, which expedites the (first) spin-flip process mediated by the spin-orbit interaction. We believe that is why the spin-relaxation in the superconducting state is more effective than that in the normal state. We thus suppose the fast increase of the spin diffusion length near T_c should be limited by its normal-state value, although it could not be confirmed in our study because of the lack of the resolution in the measurements of the spin diffusion length very close to T_c.

It is surprising that a large spin-injection effect was observed in spite of the rather small interfacial transparency in the samples A and B. As pointed out in Ref. 37, the spin injection rate through the interface of low transparency is proportional to the interfacial polarization and the ratio between the interfacial resistance and the resistance corresponding to the spin-diffusion length in the non-magnetic electrode. The interfacial polarization decreases with increasing interfacial resistance in a system with a diffusive interface as the interfacial spin-flip scattering occurs more
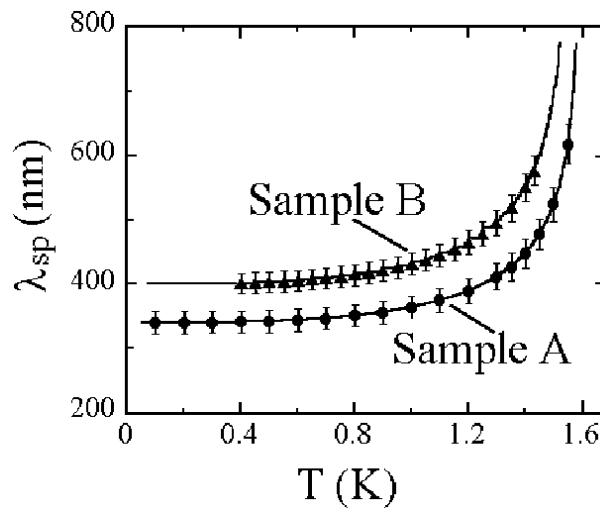

FIG. 8: The temperature dependence of λ_{sp} for the samples A (circles) and B (triangles), extracted from the best-fit curves in $I-V$ characteristics based on Eqs. (2) and (3). The solid curves are the best fits to the relation $\lambda_{sp} = \sqrt{D\tau_{sp}}$, together with Eq. (4).

frequently. But, at the same time, the ratio between the two resistance values increases with increasing the interfacial resistance. We suppose the two competing factors kept the spin-injection efficiency high enough in our systems of finite interfacial resistance close to 2.4 Ω. A quantitative estimate of the spin-injection rate, however, is not available because the first-principle calculation of the interfacial polarization with spin-flip scattering is not available.

In conclusion, we observed the suppression of the nonequilibrium superconductivity, induced by spin-polarized quasiparticle injection into mesoscopic superconducting Al wires in proximity contact with an overlaid ferromagnetic Co wire. The suppression, as evidenced by the occurrence of finite voltages for the bias-current range below the superconducting onset, was pronounced when the spin-polarized currents were injected through the Co/Al interfaces. The finite voltages in the samples with transparent interfaces of low interfacial resistances are attributed to the dynamic pair breaking by the quasiparticles with the imbalanced spin population. The temperature dependence of the spin diffusion length in a superconductor, estimated from the finite voltages over a certain length of Al wire near the interface, suggests that the spin diffusion in the superconductor is governed by the pair condensation of quasiparticles through opposite spin channels. Since the pair condensation depopulates the spin-balanced quasiparticles more efficient spin flip can take place, via the spin-orbit interaction, in the superconducting state than in the normal state, making the spin diffusion length, in general, shorter in the superconducting state.

Acknowledgments

---

[*] Present address: Electronic Devices Group, Korea Research Institute of Standards and Science

[†] Electronic address: hjlee@postech.ac.kr

[1] M. Johnson and R. H. Silsbee, Phys. Rev. Lett. **55**, 1790 (1985); Phys. Rev. B **37**, 5326 (1988).

[2] G. Prinz, Phys. Today **48**, No. 4, 58 (1995).

[3] S. Datta and B. Das, Appl. Phys. Lett. **56**, 665 (1990).

[4] J. Nitta, T. Akazaki, H. Takayanagi, and T. Enoki, Phys. Rev. Lett. **78**, 1335 (1997).

[5] P. R. Hammar, B. R. Bennett, M. J. Yang, and M. Johnson, Phys. Rev. Lett. **83**, 203 (1999).

[6] H. J. Zhu, M. Ramsteiner, H. Kostial, M. Wassermeier, H.-P. Schonherr, and K. H. Ploog, Phys. Rev. Lett. **87**, 016601 (2001).

[7] F. J. Jedema, A. T. Filip, and B. J. van Wees, Nature **410**, 345 (2001).

[8] F. J. Jedema, H. B. Heersche, A. T. Filip, J. J. A. Baselmans, and B. J. van Wees, Nature **416**, 713 (2002).

[9] F. J. Jedema, M. S. Nijboer, A. T. Filip, and B. J. van Wees, Phys. Rev. B **67**, 085319 (2000).

[10] D. Lubzens1 and S. Schultz, Phys. Rev. Lett. **36**, 1104 (1976).

[11] F. Beuneu and P. Monod, Phys. Rev. B **13**, 3424 (1976).

[12] J. Fabian and S. Das Sarma, Phys. Rev. Lett. **83**, 1211 (1999).

[13] G. Bergmann, Phys. Rev. B **29**, 6114 (1984).

[14] J. M. Gordon, C. J. Lobb, and M. Tinkham, Phys. Rev. B **28**, R4046 (1983).

[15] R. Meservey and P. M. Tedrow, Phys. Rep. **238**, 173 (1994).

[16] R. Meservey, P. M. Tedrow, and R. C. Bruno, Phys. Rev. B **11**, 4224 (1975).

[17] C. Grimaldi and P. Fulde, Phys. Rev. Lett. **77**, 2550 (1996).

[18] D. J. Monsma and S. S. P. Parkin, Appl. Phys. Lett. **77**, 720 (2000).

[19] M. Johnson, Appl. Phys. Lett. **65**, 1460 (1994).

[20] D. C. Vier and S. Schults, Phys. Lett. **98A**, 283 (1983).

[21] N. M. Nemes, J. E. Fischer, G. Baumgartner, L. Forró, T. Fehér, G. Oszlányi, F. Simon, and A. Jánossy, Phys. Rev. B **61**, 7118 (2000).

[22] T. Yamashita, S. Takahashi, H. Imamura, and S. Maekawa, Phys. Rev. B **65**, 172509 (2002).

[23] Y. Yafet, Phys. Lett. **98A**, 287 (1983).

[24] M. A. Sillanpää, T. T. Heikkilä, R. K. Lindell, and P. J. Hakonen, Europhys. Lett. **56**, 590 (2001).

[25] V. A. Vas'ko, V. A. Larkin, P. A. Kraus, K. R. Nikolaev, D. E. Grupp, C. A. Nordman, and A. M. Goldman, Phys. Rev. Lett. **78**, 1134 (1997).

[26] Z. W. Dong, R. Ramesh, and T. Venkatesan, M. Johnson, Z. Y. Chen, S. P. Pai, V. Talyansky, R. P. Sharma, R. Shreekala, C. J. Lobb, and R. L. Greene, Appl. Phys. Lett. **71**, 1718 (1997).

[27] N.-C. Yeh, R. P. Vasquez, C. C. Fu, A. V. Samoilov, Y. Li, and K. Vakili, Phys. Rev. B **60**, 10522 (1999); C.-C. Fu, Z. Huang, and N.-C. Yeh, *ibid* **65**, 224516 (2002).

[28] R. M. Stroud, J. Kim, C. R. Eddy, D. B. Chrisey, J. S. Horwitz, D. Koller, M. S. Osofsky, and R. J. Soulen, Jr., and R. C. Y. Auyeung, J. Appl. Phys. **83**, 7189 (1998).

[29] Y.-S. Shin. and H.-J. Lee, J. Kim, J. Park, and K. Char, J. Kor. Phys. Soc. **44**, 904 (2004).

[30] P. Santhanam and D. E. Prober, Phys. Rev. B**29**, 3733 (1984).

[31] For example, N. W. Ashcroft and N. D. Mermin, *Solid State Physics* (Harcourt College Publishers, Orlando 1976) p 38.

[32] M. Giroud, H. Courtois, and K. Hasselbach, D. Mailly, and B. Pannetier, Phys. Rev. B **58**, R11872 (1998).

[33] Once in this study the spin injection effect was observed over several μm range in the superconducting Al wire. Multiple leads in the sample B were arranged over an extended length of the Al wire to examine the seeming long-range character of the spin diffusion. But it has not been reproduced ever since so that the extended multiple-leads arrangement in the sample B turned out to be unnecessary. We believe the strange behavior was caused by some defects in the sample.

[34] J. H. Xu, J. L. Shen, J. H. Miller, Jr. and C. S. Ting, Phys. Rev. Lett. 73, 2492 (1994).

[35] A. Schmid and G. Schön, J. Low Temp. Phys. **20** 207 (1975).

[36] J. Fabian and S. Das Sarma, Phys. Rev. Lett. **83**, 1211 (1999).

[37] S. Takahashi and S. Maekawa, Phys. Rev. B **67**, 052409 (2003).